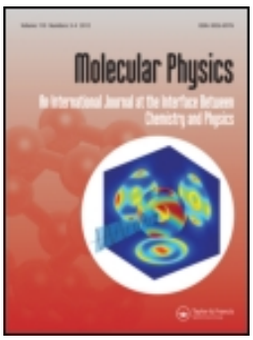

Taylor & Francis
Taylor & Francis Group

Molecular Physics

An International Journal at the Interface Between Chemistry and Physics

ISSN: 0026-8976 (Print) 1362-3028 (Online) Journal homepage: http://www.tandfonline.com/loi/tmph20

A molecular dynamics study on the role of attractive and repulsive forces in excess heat capacity at constant volume of dense fluids

Ali Morsali , S. Ali Beyramabadi , S. Hooman Vahidi & Maryam Ghorbani

To cite this article: Ali Morsali , S. Ali Beyramabadi , S. Hooman Vahidi & Maryam Ghorbani (2012) A molecular dynamics study on the role of attractive and repulsive forces in excess heat capacity at constant volume of dense fluids, Molecular Physics, 110:8, 483-490, DOI: 10.1080/00268976.2012.655795

To link to this article: http://dx.doi.org/10.1080/00268976.2012.655795

Accepted author version posted online: 10 Jan 2012.
Published online: 30 Jan 2012.

Molecular Physics
Vol. 110, No. 8, 20 April 2012, 483–490

Taylor & Francis
Taylor & Francis Group

RESEARCH ARTICLE

A molecular dynamics study on the role of attractive and repulsive forces in excess heat capacity at constant volume of dense fluids

Ali Morsali*, S. Ali Beyramabadi, S. Hooman Vahidi and Maryam Ghorbani

Department of Chemistry, Mashhad Branch, Islamic Azad University, Mashhad, Iran

(*Received 20 October 2011; final version received 24 December 2011*)

The curves of experimental heat capacity against density show a minimum around and below the critical temperature (Tc), but at higher temperatures, this minimum is not observed. In this study, the role of attractive and repulsive forces on excess heat capacity of Lennard–Jones (LJ) dense fluids has been investigated using a molecular dynamics simulation technique. LJ potential is divided into attractive and repulsive parts. From the molecular dynamics calculations, potential energy and heat capacities have been obtained for Argon at temperatures of 100–500 K. The repulsive forces play the main role in causing the heat capacities at temperatures greater than critical point. Around and below the critical temperature, the role of repulsion is dominant at high densities, but attraction has the main role at low densities, consequently at middle densities, a minimum is formed.

Keywords: molecular dynamics; heat capacity; attractive; repulsive; dense fluid

1. Introduction

Among the quantities high importance are the heat capacities, which have been extensively tabled for different substances due to ease of experimental measurement. The importance of heat capacities is stressed in every text book on thermodynamics. Heat capacities are used for calculation of many thermodynamic quantities, the most important of which are change in enthalpy, change in internal energy, change in entropy and Joule–Thomson coefficient [1].

According to statistical mechanics, the internal energy of a body, E, consist of the sum of the kinetic energy, $K(T)$, of molecules comprising the system due to molecular motions plus intermolecular attractive, U_A, and repulsive, U_R, energies [1]:

$$E = K(T) + U_A + U_R \tag{1}$$

and

$$U = U_A + U_R \tag{2}$$

where U is the total intermolecular potential energy of the body.

The temperature dependence of the internal energy (E) is given by the heat capacity at constant volume (C_V) at a given temperature, formally defined by

$$C_V = \left(\frac{\partial E}{\partial T}\right)_V \tag{3}$$

where E and V are internal energy and molar volume, respectively.

Differentiation of Equation (1) with respect to temperature at constant volume gives:

$$\left(\frac{\partial E}{\partial T}\right)_V = \left(\frac{\partial KE}{\partial T}\right)_V + \left(\frac{\partial U_R}{\partial T}\right)_V + \left(\frac{\partial U_A}{\partial T}\right)_V \tag{4}$$

Equation (4) can be written as:

$$C_V = C_{V,KE} + C_{V,R} + C_{V,A} \tag{5}$$

where $C_{V,KE}$, $C_{V,A}$ and $C_{V,R}$ are heat capacities resulting from kinetic energy, attractive and repulsive intermolecular interactions, respectively.

Excess heat capacity, C_v^{ex}, is defined as:

$$C_V^{ex} = C_V - C_{V,KE} = C_{V,R} + C_{V,A} \tag{6}$$

Clearly, C_V^{ex}, is related to that part of the internal energy that is due to intermolecular potential energies. The purpose of this study is to investigate the role of attractive and repulsive intermolecular energies on behaviour of excess heat capacity using a molecular dynamics simulation. Other thermodynamic properties have been evaluated using this method [2,3].

To further confirm the accuracy of MD simulations, these results have been compared with other independent sources. For this purpose, two accurate analytic equations of state for the LJ fluid [4–6], MD results [7] and experimental data [8] were used.

*Corresponding author. Email: almorsali@mshiau.ac.ir (Morsali)

ISSN 0026–8976 print/ISSN 1362–3028 online

http://dx.doi.org/10.1080/00268976.2012.655795
http://www.tandfonline.com

2. Theory

From the radial distribution function theory of dense fluids, C_V^{ex} could be calculated from the following equation [9]:

$$C_V^{ex} = 2\pi N\rho \int_0^{\infty} u(r)\left(\frac{\partial g(r,\rho,T)}{\partial T}\right)_{r,V} r^2\,\mathrm{d}r \qquad (7)$$

Because

$$E^{ex} = 2\pi N\rho \int_0^{\infty} u(r)\,g(r,\rho,T) r^2\,\mathrm{d}r \qquad (8)$$

where $g(r,\rho,T)$, $u(r)$, ρ, r and E^{ex} are radial distribution function, interparticle pair potential, molar density, interparticle distance and excess internal energy, respectively.

For the evaluation of heat capacities, differential like $(\partial g(r,\rho,T)/\partial T)_{r,\rho}$ is required. Several expressions for analytical $g(r,\rho,T)$ have been presented by fitting to simulation data [10–12]. Analytical radial distribution functions have been used for the calculation of different thermodynamic properties [9,13–17].

By separating the role of attractive and repulsive forces, there is no possibility for the calculation of above integral. This is due to the unavailability of an analytical expression for the radial distribution function and therefore there is no other alternative except using molecular dynamics.

In our molecular simulation study, we choose the Lennard–Jones (LJ) intermolecular potential energy function to represent the interaction between simple molecules, like argon, krypton, and xenon. The reason for the choice of the LJ potential function is that it is shown to be an effective potential representing a statistical average of the true pair and many-body interactions in simple molecular systems. The LJ intermolecular potential energy function can be divided into attractive and repulsive parts as is shown below [18–20]:

$$u_{LJ}(r) = 4\varepsilon\left[\left(\frac{\sigma}{r}\right)^{12} - \left(\frac{\sigma}{r}\right)^{6}\right] \qquad (9)$$

$$u_{LJA}(r) = \begin{cases} r \geq r_m & u_{LJ}(r) \\ r < r_m & -\varepsilon \end{cases} \qquad (10)$$

$$u_{LJR}(r) = \begin{cases} r \geq r_m & 0 \\ r < r_m & u_{LJ}(r) + \varepsilon \end{cases} \qquad (11)$$

where $u_{LJ}(r)$, $u_{LJR}(r)$, $u_{LJA}(r)$, ε, σ, and r_m are LJ potential function, LJ repulsive part, LJ attractive part, minimum energy parameter, length parameter and position of minimum, respectively.

Weeks *et al.* (WCA) [18] first introduced splitting of the Lennard–Jones intermolecular potential given in Equations (9)–(11). They established that the equilibrium structure of a liquid is primarily determined by the repulsive part of the potential. Several works have been presented to show the role of interparticle forces (attractive and repulsive) in thermodynamic parameters [2,3,19–24].

Molecular dynamics results (our work) are compared with Kolafa and Nezbeda equation of state (KN) [4] and Mecke *et al.* equation of state [5,6]. The equations related to KN EOS are as follows

$$\frac{P^*}{\rho^* T^*} = z_{HS} + \rho(1 - 2\gamma\rho*^2)\exp(-\gamma\rho*^2)\Delta B_{2,hBH} + \sum_{ij} jC_{ij}(T^*)^{i/2-1}(\rho^*)^j \qquad (12)$$

$$E^* = \frac{3(z_{HS}-1)}{d_{hBH}}\frac{\partial d_{hBH}}{\partial(1/T^*)} + \rho\exp(-\gamma\rho*^2)\frac{\partial \Delta B_{2,hBH}}{\partial(1/T^*)} - \sum_{ij}(i/2-1)\,C_{ij}(T^*)^{i/2}(\rho^*)^j \qquad (13)$$

where z_{HS} is

$$z_{HS} = \frac{P^*_{HS}}{\rho^* T^*} = \frac{1+\eta+\eta^2-\eta^3(2/3)(1+\eta)}{(1-\eta)^3} \qquad (14)$$

with $\eta = \pi(\rho^*)^3 d^3_{hBH}/6$ and $E^* = E/N\varepsilon$, $P^* = P\sigma^3/\varepsilon$, $T^* = kT/\varepsilon$ $\rho^* = \rho\sigma^3$ are reduced internal energy, pressure, temperature and density, respectively. Functions d_{hBD} and $\Delta B_{2,hDB}$ are approximated by the following equation with coefficients given in Ref. (4).

$$f(T^*) = \sum_i C_i T^{*\,i/2} + C_{\ln}\ln(T^*); \qquad f(T^*) = (d_{hBH}, \Delta B_{2,hBH}) \qquad (15)$$

d_{hBD} and $\Delta B_{2,hDB}$ derivatives over $1/T$ are

$$\frac{\partial f(T^*)}{\partial(1/T^*)} = -T^*\left(\sum_i \frac{i}{2} C_i T^{*\,i/2} + C_{\ln}\right) \qquad (16)$$

The equations related to Mecke *et al.* EOS [5–6] are as follows

$$F = F_H + F_A \qquad (17)$$

where F is residual Helmholtz energy. F_H accounts for the hard-body interaction and F_A for the attractive dispersion forces.

For a system of hard spheres with a packing fraction ξ the residual Helmholtz energy F_H is given according to Carnahan and Starling [25] as

$$\frac{F^*_H}{T^*} = \frac{(4\xi - 3\xi^2)}{(1-\xi)^2} \qquad (18)$$

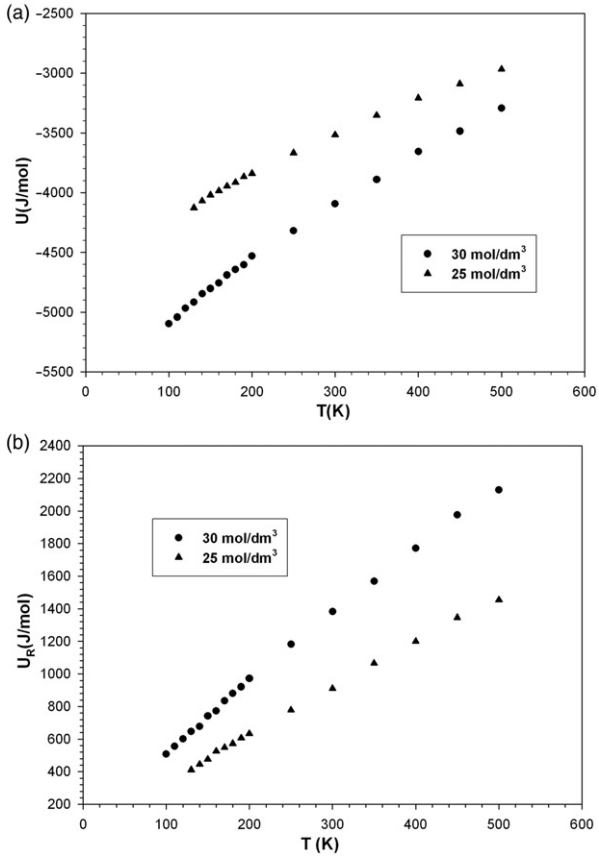

Figure 1. Potential energy of argon versus temperature. In this figure (a) U is the MD data using LJ potential at $30\,\mathrm{mol\,dm^{-3}}$ (•) and $25\,\mathrm{mol\,dm^{-3}}$ (▲), (b) U_R is the contribution of LJ repulsive potential at $30\,\mathrm{mol\,dm^{-3}}$ (•) and $25\,\mathrm{mol\,dm^{-3}}$ (▲).

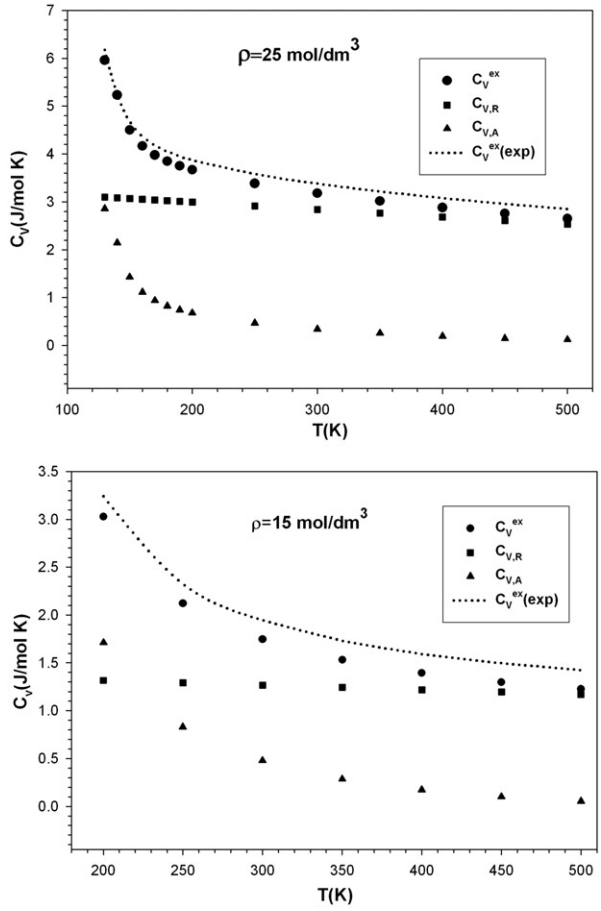

Figure 2. Heat capacity versus temperature at 25 and $15\,\mathrm{mol\,dm^{-3}}$. In this figure C_V^{ex} is the excess heat capacity using LJ potential (•), $C_{V,R}$ is the contribution of LJ repulsive potential (■), $C_{V,A}$ is the contribution of LJ attractive potential (▲) and C_V^{ex}(exp) is the experimental excess heat capacity (. . . .) [8].

where $F_H^* = F_H/N\varepsilon$ and

$$\xi = 0.1617(\rho^*/\rho_c^*)\left[0.689 + 0.311(T^*/T_c^*)^{0.3674}\right]^{-1} \tag{19}$$

where $\rho_c^* = 0.3107$ and $T_c^* = 1.328$ are the critical density and temperature, respectively.

F_A is presented by the following equation with powers (m_i, n_i, p_i and q_i) and coefficients (c_i) given in Reference (5–6).

$$\frac{F_A^*}{T^*} = \sum_i c_i (T^*/T_c^*)^{m_i} (\rho^*/\rho_c^*)^{ni} \exp[p_i(\rho^*/\rho_c^*)^{q_i}] \tag{20}$$

where $F_A^* = F_A/N\varepsilon$.

Reduced heat capacities ($C_V^* = (\partial E^*/\partial T^*)_{\rho^*} = -T^*(\partial^2 F^*/\partial T^{*2})_{\rho^*} = C_V/Nk$) have been converted to SI units ($\mathrm{J\,mol^{-1}\,K^{-1}}$) using $\sigma = 3.405\,\text{Å}$ and $\varepsilon/k = 119.8\,\mathrm{K}$ for Argon.

3. Results and discussion

Thermodynamic differential properties such as heat capacities are classified in thermodynamic response functions group [26]. Two general methods are available for evaluating such properties. In the first method we use several simulations to determine values of the simple quantity (E in the case of C_V) as a function of the independent variable (T for C_V). We then compute the response function separately from the simulations, either by numerical differentiation or by analytically differentiating an empirical fit to the simulation results for E. In the second method, we evaluate the derivative analytically via statistical mechanics [7]. The analytical form for the derivative always involves a fluctuation. Meier *et al.* [7] used the following equation to calculate the heat capacity:

$$C_V = (\partial^2 S/\partial E^2)_V^{-1} = k(1 - \Omega_{00}\Omega_{20})^{-1} \tag{21}$$

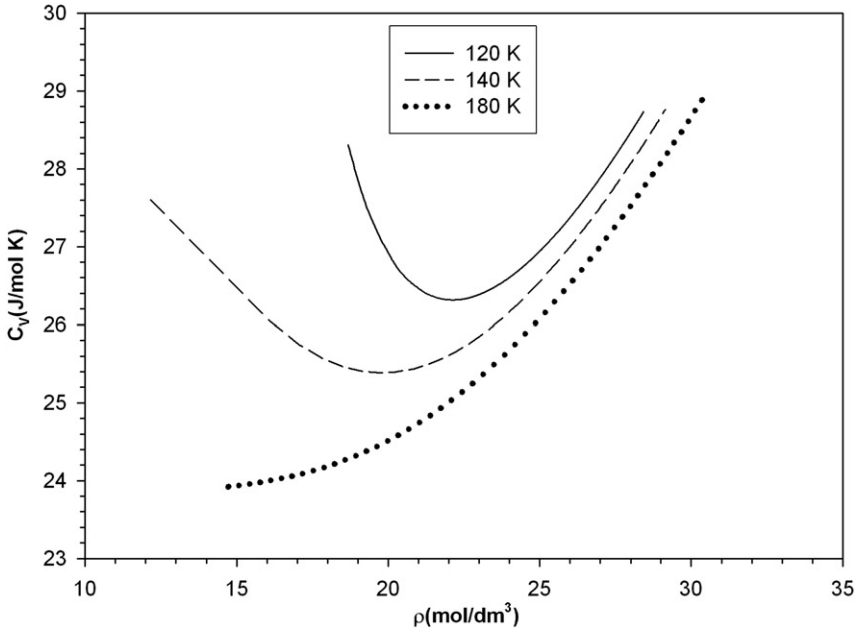

Figure 3. Experimental heat capacity (C_V(exp)) against ρ for Nitrogen ($T_C = 126.2$ K).

where $\Omega_{mn} = (1/\omega)(\partial^{m+n}\Omega/\partial E^m \partial V^n)$. An isolated system in classical statistical thermodynamics is characterized by the phase space volume Ω and the phase space density ω (Equations (2.17) and (2.18) of Ref. 7).

Of these two methods, the first is often more accurate than the second, but the first has the disadvantage that several simulations must be done before the derivative can be estimated. The second method produces an estimate for the derivative from a single simulation.

We used the first method. The molecular dynamics calculations have been performed for 5000 argon atoms interacting via the Lennard–Jones potential ($\sigma = 3.405$ Å, $\varepsilon/k = 119.8$ K). The periodic boundary conditions (PBC) were applied to molecular dynamics calculations (MD) as usual. The NVT ensemble was implemented using the Nose–Hoover thermostat. Number of time steps, size of time step, and cutoff (r_{cutoff}) of the interatomic potential are 5000, 0.01 ps, and 2.5σ, respectively. In the present study, all calculations due to simulation have been performed using the MOLDY software [27]. The Lennard–Jones potential is supported and the code is structured to give a straightforward interface to add a new functional form. We have added $u_{LJR}(r)$ and $u_{LJA}(r)$ into the Moldy simulation program. Molecular dynamics calculations have been performed to obtain U and U_R at temperatures of 100–500 K and constant densities of 15–35 mol dm^{-3} considering $u_{LJ}(r)$ and $u_{LJR}(r)$, respectively. Figure 1 shows the results of this calculation at constant densities of 30 and 25 mol dm^{-3}.

Differentiation of the potential energies with respect to temperature at constant densities gives C_V^{ex}, $C_{V,R}$ and $C_{V,A} = C_V - C_{V,R}$ as shown in Figure 2 at densities of 25 and 15 mol dm^{-3}. Table 1 represents these results at constant densities of 35, 30 and 20 mol dm^{-3}.

In this table, these quantities (C_V^{ex}) are compared with the Kolafa and Nezbeda equation of state (KN EOS) [4], Mecke *et al.* equation of state [5,6], MD results (Meier *et al.*) [7] and experimental data (exp) [8].

If experimental data (exp)are taken as the criteria for comparison, the values of average absolute deviations (AAD) in connection with our work (MD), KN EOS (Equations (12)–(16)), Mecke *et al.* EOS (Equations (17)–(20)) and Meier *et al.* (by fitting to the MD data of table D.1 of Ref. 7) are 3.82, 5.74, 5.93 and 4.66, respectively. As it is seen from the AAD values, MD results well predict the values of $C_{V,(\text{exp})}^{ex}$.

$$AAD = \frac{1}{n}\sum_{i=1}^{n} 100 \times \frac{\left|C_{V,i(\text{exp})}^{ex} - C_{V,i(MD \text{ or } EOS)}^{ex}\right|}{C_{V,i\,\text{exp}}^{ex}} \quad (22)$$

As shown in Figure 2 and Table 1, with increasing the density, the role of repulsive forces in determining of heat capacity increases, so that at all densities higher than 25 mol dm^{-3}, the repulsive forces are dominant. With decreasing density, at temperatures around and below the critical temperature, the role of attractive forces considerably increases, so that at these temperatures and at densities below 25 mol dm^{-3}, the role of

Table 1. Potential energy ($J\,mol^{-1}$) obtained from LJ potential (U), experimental (U_{exp}), contribution of LJ repulsive potential (U_R) and contribution of LJ attractive potential (U_A). C_V^{ex}, $C_{V,R}$, $C_{V,A}$, C_V^{ex}(exp), $C_V^{ex}(Meier)$, $C_V^{ex}(KN)$ and $C_V^{ex}(Mecke)$ are excess heat capacities ($J\,mol^{-1}K^{-1}$) using LJ potential (our work), LJ repulsive potential, LJ attractive potential, experimental data, Meier *et al.* (MD), KN EOS and Mecke *et al.* EOS, respectively.

T (K)	U	U_{exp}	U_R	U_A	C_V^{ex}	$C_{V,R}$	$C_{V,A}$	C_V^{ex}(exp)	$C_V^{ex}(Meier)$	$C_V^{ex}(KN)$	$C_V^{ex}(Mecke)$
$\rho = 35\,mol/dm^3$											
100	−5883.1	−5679.1	789.0	−6672.1	7.62	6.79	0.82	8.12	8.38	8.61	8.56
110	−5782	−5598.7	868.4	−6650.4	7.54	6.73	0.81	7.96	8.16	8.26	8.26
120	−5704.6	−5519.9	930.9	−6635.5	7.47	6.67	0.80	7.79	7.96	8.01	8.04
130	−5593.2	−5442.9	996.6	−6589.8	7.40	6.61	0.79	7.63	7.76	7.81	7.86
140	−5550.9	−5367.3	1063.4	−6614.3	7.33	6.55	0.78	7.50	7.58	7.64	7.69
150	−5499.5	−5292.8	1114.6	−6614.1	7.26	6.49	0.76	7.39	7.41	7.49	7.53
160	−5395.2	−5219.3	1201.5	−6596.7	7.19	6.43	0.75	7.32	7.25	7.35	7.38
170	−5344.1	−5146.4	1252.8	−6596.9	7.11	6.37	0.74	7.25	7.17	7.21	7.23
180	−5244.5	−5074.2	1310	−6554.5	7.04	6.32	0.73	7.20	7.01	7.09	7.10
190	−5170.2	−5002.4	1398.9	−6569.1	6.97	6.26	0.71	7.16	6.9	6.97	6.97
200	−5115.4	−4931.0	1436.9	−6552.3	6.90	6.20	0.70	7.11	6.81	6.86	6.85
250	−4815.9	−4581.1	1737.9	−6553.8	6.54	5.90	0.64	6.87	6.39	6.37	6.35
300	−4506.4	−4244.8	2050.7	−6557.09	6.18	5.60	0.58	6.57	6.1	5.99	5.97
350	−4156.6	−3924.6	2296.9	−6453.51	5.82	5.30	0.52	6.24	5.73	5.69	5.67
400	−3914.0	−3620.8	2582.0	−6496.0	5.47	5.00	0.46	5.91	5.6	5.44	5.43
450	−3585.8	−3332.8	2772.2	−6358.0	5.11	4.71	0.40	5.61	5.2	5.24	5.23
500	−3393.7	−3059.3	3050.0	−6443.7	4.75	4.41	0.34	5.33	5.13	5.06	5.06
$\rho = 30\,mol/dm^3$											
100	−5097.0	−4932.9	508.6	−5605.6	6.29	4.72	1.57	6.35	6.48	6.81	6.52
110	−5042.2	−4868.4	554.7	−5596.9	6.17	4.69	1.48	6.15	6.14	6.16	5.96
120	−4969.0	−4809.0	601.3	−5570.3	6.04	4.66	1.38	5.79	5.77	5.78	5.67
130	−4918.0	−4752.0	646.1	−5564.1	5.91	4.62	1.29	5.63	5.56	5.54	5.50
140	−4848.0	−4696.1	678.5	−5526.5	5.79	4.59	1.19	5.55	5.4	5.38	5.38
150	−4803.0	−4641.0	742.0	−5545.0	5.66	4.56	1.10	5.48	5.31	5.25	5.28
160	−4756.8	−4586.5	773.6	−5530.4	5.54	4.53	1.01	5.42	5.2	5.16	5.19
170	−4689.9	−4532.5	835.7	−5525.6	5.41	4.49	0.91	5.36	5.12	5.07	5.11
180	−4643.4	−4479.2	880.2	−5523.6	5.28	4.46	0.82	5.31	5.03	5.00	5.04
190	−4602.8	−4426.4	920.4	−5523.2	5.20	4.43	0.77	5.25	4.98	4.93	4.96
200	−4529.9	−4374.2	972.4	−5502.3	5.15	4.40	0.75	5.20	4.93	4.87	4.89
250	−4319.4	−4120.6	1181.9	−5501.3	4.90	4.24	0.67	4.95	4.63	4.59	4.59
300	−4094.1	−3878.9	1381.7	−5475.8	4.67	4.07	0.60	4.72	4.41	4.37	4.35
350	−3889.6	−3648.4	1568.7	−5458.3	4.45	3.91	0.54	4.50	4.22	4.18	4.16
400	−3655.1	−3428.5	1770.4	−5425.5	4.25	3.75	0.50	4.30	4.08	4.03	4.01
450	−3485.7	−3218.5	1976.3	−5462.0	4.06	3.59	0.47	4.11	3.95	3.90	3.88
500	−3292.5	−3017.5	2128.9	−5421.4	3.88	3.43	0.46	3.93	3.82	3.78	3.77
$\rho = 20\,mol/dm^3$											
140	−3316.4	–	281.5	−3597.9	6.10	2.07	4.03	–	4.8	5.47	6.11
150	−3261.2	−3228.3	311.8	−3573.0	5.60	2.07	3.53	–	4.21	4.71	5.05
160	−3211	−3165.2	325.5	−3536.5	5.10	2.06	3.04	5.43	3.81	4.16	4.31
170	−3199.2	−3116.5	346.6	−3545.8	4.60	2.06	2.54	4.41	3.47	3.74	3.80
180	−3162.9	−3075.5	365.6	−3528.5	4.10	2.05	2.05	3.85	3.22	3.43	3.42
190	−3130.2	−3038.7	384.9	−3515.1	3.67	2.04	1.63	3.52	3.07	3.19	3.15
200	−3103.3	−3004.7	402.7	−3506.0	3.45	2.04	1.41	3.30	2.51	3.00	2.94
250	−2960.5	−2855.3	510.2	−3470.7	2.91	2.01	0.90	2.76	2.27	2.46	2.41
300	−2854.7	−2724.5	613.7	−3468.4	2.65	1.98	0.67	2.50	2.15	2.23	2.20
350	−2739.1	−2604.2	707.5	−3446.6	2.48	1.95	0.53	2.33	2.07	2.10	2.08
400	−2639.7	−2491.0	804.8	−3444.5	2.35	1.92	0.44	2.20	2.01	2.01	2.00
450	−2541.5	−2383.2	895.0	−3436.5	2.26	1.88	0.38	2.11	1.97	1.95	1.94
500	−2455.9	−2279.7	995.8	−3451.7	2.18	1.85	0.33	2.03	4.8	1.90	1.89

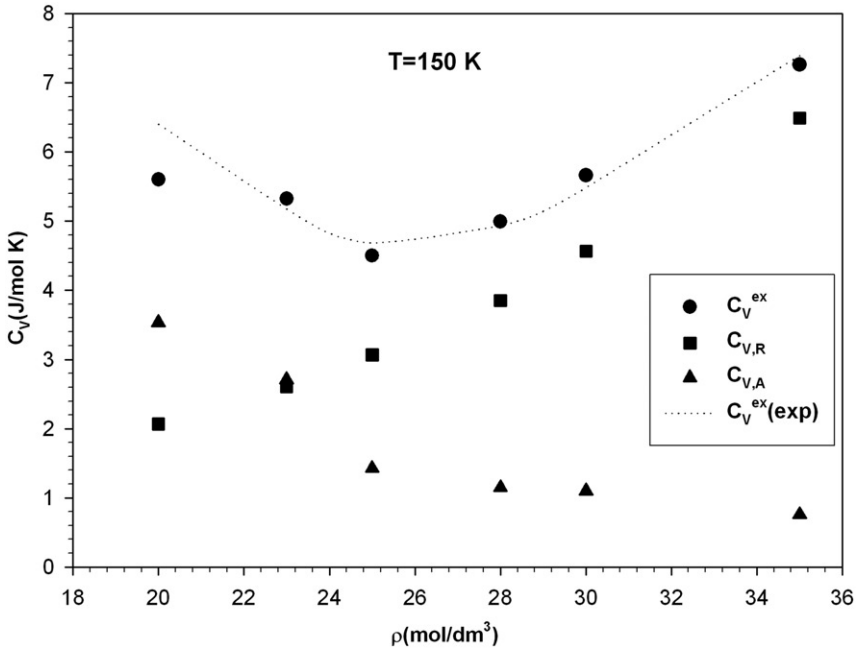

Figure 4. Heat capacity versus density at 150 K. The caption is the same as Figure 2.

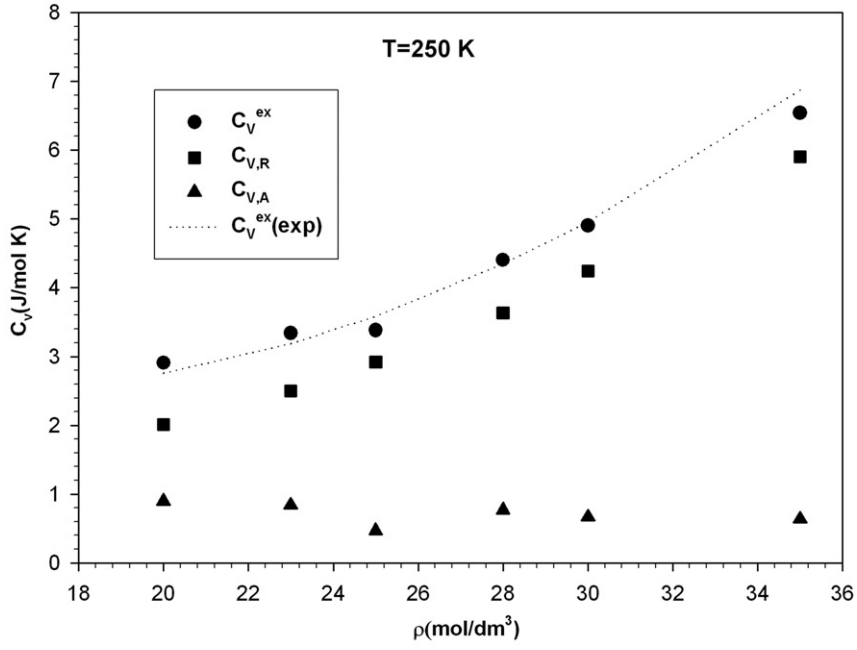

Figure 5. Same as Figure 4 but at 250 K.

attractive forces becomes dominant. Although at higher temperatures (especially higher than 200 K), again the repulsive forces are dominant.

If the curves of experimental heat capacity (C_V(exp)) against ρ are plotted at temperatures around and below the critical temperature for Argon, a minimum will appear which is not observed at higher temperatures. This behaviour is not unique to a LJ fluid such as Argon. Figure 3 shows this minimum for Nitrogen ($T_C = 126.2$ K) [28]. This phenomenon could be justified with regard to the role of attractive and repulsive forces.

Table 2. Heat capacities at 130, 140, 160 and 170 K. The caption is the same as Figure 2.

ρ(mol/dm^3)	C_V^{ex}	$C_{V,R}$	$C_{V,A}$	C_V^{ex}(exp)
$T=130$ K				
25	5.96	3.1	2.86	6.18
28	5.37	3.89	1.48	5.31
30	5.91	4.62	1.29	5.36
35	7.4	6.61	0.79	7.63
$T=140$ K				
23	6.6	2.62	3.99	6.45
25	5.23	3.09	2.14	5.24
28	5.13	3.87	1.26	5.07
30	5.79	4.59	1.19	5.55
35	7.33	6.55	0.78	7.5
$T=160$ K				
20	5.1	2.06	3.04	5.43
23	4.61	2.6	2.02	4.46
25	4.17	3.05	1.11	4.37
28	4.9	3.82	1.07	4.84
30	5.54	4.53	1.01	5.42
35	7.19	6.43	0.75	7.32
$T=170$ K				
20	4.60	2.06	2.54	4.41
23	4.22	2.59	1.63	4.07
25	3.98	3.04	0.94	4.18
28	4.83	3.80	1.02	4.77
30	5.41	4.49	0.91	5.36
35	7.11	6.37	0.74	7.25

Figure 4 shows this minimum for Argon at 150 K. Table 2 presents the values of C_V^{ex}, $C_{V,A}$and $C_{V,R}$ at 130–170 K. As it is observed, at high densities around and below the critical temperature, the contribution of repulsion ($C_{V,R}$) is dominant, while at low densities, the contribution of attraction ($C_{V,A}$) plays the main role. Therefore, at middle densities, a minimum appears. At higher temperatures (especially higher than 200 K), this minimum is not observed and the contribution of repulsion ($C_{V,R}$) is completely dominant. Figure 5 shows C_V versus ρ at temperature 250 K.

4. Conclusions

The contribution of attractive and repulsive forces in determining the excess heat capacity of LJ dense fluids has been studied. LJ potential has been divided into repulsive and attractive parts and the heat capacity was calculated using these potentials. In general, with increasing density and temperature, the contribution of repulsion will increase. With decreasing density, around and below the critical point, the contribution of attraction will considerably increase.

It means that if we plot heat capacity versus density at constant temperature (around the critical temperature), at high densities the contribution of repulsion and at low densities the contribution of attraction are considerable, while at middle densities, reduction is observed in both cases and consequently a minimum appears in the heat capacity curve. At higher temperatures due to complete dominance of the repulsion forces with increasing density, heat capacity is increased and no minimum is observed.

The above description applies to heat capacity at constant volume, which could be expanded to heat capacity at constant pressure, being related to such important quantities as Joule-Thompson Coefficient and is the subject of our future investigations.

Acknowledgements

We gratefully acknowledge financial support from the islamic azad university, Mashhad branch (Grant Number: 89291\302\41).

References

[1] I.N. Levine, *Physical Chemistry* (McGraw Hill, New York, 2002).
[2] E.K. Goharshadi, A. Morsali and G.A. Mansoori, Chem. Phys. **331**, 332 (2007).
[3] J.E. Straub, Mol. Phys. **76**, 373 (1992).
[4] J. Kolafa and I. Nezbeda, Fluid Phase Equilib. **100**, 1 (1994).
[5] M. Mecke, A. Muller, J. Winkelmann, J. Vrabec, J. Fischer, R. Span and W. Wagner, Int. J. Thermophys. **17**, 391 (1996).
[6] M. Mecke, A. Muller, J. Winkelmann, J. Vrabec, J. Fischer, R. Span and W. Wagner, Erratum, Int. J. Thermophys. **19**, 1493 (1998).
[7] M. Meier, PhD thesis, University of the Federal Armed Forces, Hamburg (2002).
[8] R.B. Stewart and R.T. Jacobsen, J. Phys. Chem. Ref. Data **18**, 639 (1989).
[9] J.S. Emampour, A. Morsali and S.A. Beyramabadi, J. Theor. Comput. Chem. **8**, 943 (2009).
[10] S. Goldman, J. Phys. Chem. **83**, 3033 (1979).
[11] E. Matteoli and G.A. Mansoori, J. Chem. Phys. **103**, 4672 (1995).
[12] A. Morsali, E.K. Goharshadi, G.A. Mansoori and M. Abbaspour, Chem. Phys. **310**, 11 (2005).
[13] A. Morsali, E.K. Goharshadi and N. Shahtahmasbi, Chem. Phys. **322**, 377 (2006).
[14] A. Morsali, S.A. Beyramabadi and M.R. Bozorgmehr, Chem. Phys. **335**, 194 (2007).
[15] J.S. Emampour, A. Morsali and A. Azaripoor, Phys. Chem. Liq. **48**, 50 (2010).
[16] C.A. Galan, A. Mulero and F. Cuadros, Mol. Phys. **103**, 527 (2005).

[17] C.A. Galan, A. Mulero and F. Cuadros, Mol. Phys. **104**, 2457 (2006).
[18] J.D. Weeks, D. Chandler and C. Andersen, J. Chem. Phys. **54**, 5237 (1971).
[19] F. Cuadros, A. Mulero and C.A. Faundez, Mol. Phys. **98**, 899 (2000).
[20] F. Cuadros, A. Mulero and W. Ahumada, Mol. Phys. **85**, 207 (1995).
[21] F. Cuadros, A. Mulero and W. Okrasinski, Physica A **223**, 321 (1996).
[22] L.A.F. Coelho, J.V. de Oliveira, F.W. Tavares and M.A. Matthews, Fluid Phase Equilibr. **194–197**, 1131 (2002).
[23] S.D. Bembenek and G. Szamel, J. Phys. Chem. B **104**, 10647 (2000).
[24] D. Plackor and R.J. Sadus, Fluid Phase Equilib. **134**, 77 (1997).
[25] N.F. Carnahan and K.E. Starling, J. Chem. Phys. **51**, 635 (1969).
[26] J.M. Haile, *Molecular Dynamics Simulation* (John Wiley & Sons, New York, 1992).
[27] The MOLDY program was coded by K. Refson, and can be downloaded from the internet at <http://www.earth.ox.ac.uk/%7Ekeith/moldy.html>.
[28] R.T. Jacobsen, R.B. Stewart and M. Jahangiri, J. Phys. Chem. Ref. Data **15**, 735 (1986).